Journal of Hydrology: Regional Studies 4 (2015) 15–35

Contents lists available at ScienceDirect

Journal of Hydrology: Regional Studies

journal homepage: www.elsevier.com/locate/ejrh

Satellite-derived surface and sub-surface water storage in the Ganges–Brahmaputra River Basin

Fabrice Papa[a,b,*], Frédéric Frappart[c,d], Yoann Malbeteau[e], Mohammad Shamsudduha[f], Venugopal Vuruputur[g,h], Muddu Sekhar[i], Guillaume Ramillien[j], Catherine Prigent[k], Filipe Aires[k,l], Rajesh Kumar Pandey[m], Sujit Bala[n], Stephane Calmant[a]

[a] *Institut de Recherche pour le Developpement, LEGOS, IRD/CNES/CNRS/UPS, Toulouse, France*
[b] *IFCWS, Indo-French Cell for Water Sciences, IRD-IISc Joint International Laboratory, Indian Institute of Science, Bangalore, India*
[c] *Université de Toulouse, UPS, OMP-GET (UPS), Toulouse, France*
[d] *Université de Toulouse, UPS, OMP-LEGOS (UPS), Toulouse, France*
[e] *Université de Toulouse, CESBIO, Toulouse, France*
[f] *Institute for Risk and Disaster Reduction, University College London, London, UK*
[g] *Center for Oceanic and Atmospheric Sciences, Indian Institute of Science, Bangalore, India*
[h] *Divecha Center for Climate Change, Indian Institute of Science, Bangalore, India*
[i] *Department of Civil Engineering and IFCWS, Indo-French Cell for Water Sciences, Indian Institute of Science, Bangalore, India*
[j] *CNRS, Géosciences Environement Toulouse, OMP-GET, Toulouse, France*
[k] *LERMA, CNRS, Observatoire de Paris, Paris, France*
[l] *Estellus, Paris, France*
[m] *CSIR – National Geophysical Research Institute (NGRI), Hyderabad, India*
[n] *Institute of Water and Flood Management, Bangladesh University of Engineering and Technology, Dhaka, Bangladesh*

ARTICLE INFO

Article history:
Received 14 October 2014
Accepted 8 March 2015
Available online 18 April 2015

Keywords:
Ganges–Brahmaputra
Surface water storage

ABSTRACT

Study region: The Ganges–Brahmaputra (GB), a major river basin of the Indian Sub-Continent (ISC), is the host of more than 700 millions people.
Study focus: In addition to monsoons and strong climate variability, GB is facing growing demands for freshwater availability by a continually growing population and rapidly developing of

* Corresponding author at: Institut de Recherche pour le Developpement, LEGOS, IRD/CNES/CNRS/UPS, Toulouse, France. Tel.: +91 7760860411.
E-mail address: fabrice.papa@ird.fr (F. Papa).

http://dx.doi.org/10.1016/j.ejrh.2015.03.004

Sub-surface water storage
Remote sensing
ENVISAT altimetry
GRACE

agricultural and industrial sectors. The management of water resources is thus of highest priority and, in the context of current over-abstraction of groundwater, accurate estimates of terrestrial freshwater storage are essential. We propose a multi-satellite approach to estimate surface freshwater storage (SWS) and subsurface water storage (SSWS, groundwater + soil moisture) variations over GB. Basin-scale monthly SWS variations for the period 2003–2007 show a mean annual amplitude of ~410 km^3, contributing to about 45% of the Gravity Recovery And Climate Experiment (GRACE)-derived total water storage variations (TWS). During the drought-like conditions in 2006, we estimate that the SWS deficit over the entire GB basin in July–August–September was about 30% as compared to other years. The SWS variations are then used to decompose the GB GRACE-derived TWS and isolate the variations of SSWS whose mean annual amplitude is estimated to be ~550 km^3. This new dataset of water storage variations represent an unprecedented source of information for hydrological and climate modeling studies of the ISC.

1. Introduction

Terrestrial waters, despite being less than 1% of the total amount of water on Earth's ice-free land, are not only essential for life and human environment, but also play a major role in climate variability. Freshwater on land is stored in various reservoirs, including ice and snow, glaciers and ice caps, aquifers and soils, and surface waters, comprising of rivers, lakes, man-made reservoirs, wetlands and seasonally inundated areas. Terrestrial water is thus an integral part of the climate system as it continuously exchange with the atmosphere and the oceans. Understanding the flow, spatial distribution, storage and variability of freshwater on land is thus fundamental to study the global water cycle, as well as for the management of water resources (Chahine, 1992; Kundzewicz et al., 2007).

An improved description of the components of the global water cycle is now recognized as being of major importance; however the distribution and spatio-temporal variations of terrestrial water storage are still poorly known at regional-to-global scale (Alsdorf et al., 2007; Papa et al., 2010a, 2013; Frappart et al., 2012). It leaves open several basic questions regarding the land surface water budget: how much freshwater is stored at the surface/sub-surface of continents? What are the spatial and temporal dynamics of terrestrial water storage and how are these linked to climate variability and anthropogenic pressure?

These questions are fundamental to understand the water cycle of the Indian Sub-Continent (ISC), a region that occupies ~4% of the world's land area, supports ~25% of the global population, and whose biophysical environment and economic development are crucially dependent on water availability (Hoekstra et al., 2012).

In particular, the ISC is drained by three of the largest river systems in the world, the Ganges, the Brahmaputra and the Indus. On its own, the Ganges, Brahmaputra and Meghna river basin (hereafter referred to as the Ganges–Brahmaputra basin or GB, Fig. 1) covers an area more than 1.7 million km^2, across India, China, Nepal, Bhutan and Bangladesh, and the combined basin hosts more than 700 million people. It is the third largest freshwater outlet to the world's oceans, being exceeded only by the Amazon and the Congo River systems (Chowdhury and Ward, 2004). It accounts for <25% of the total amount of freshwater received annually by the Bay of Bengal, which has a significant influence on the regional climate (Sengupta et al., 2006).

The GB river basin is unique in the world in terms of its climate and great availability of freshwater that is highly seasonal and driven primarily by monsoonal rainfall (Chowdhury and Ward, 2004; Papa et al., 2010b, 2012a). The basin is facing strong climate variability with alternate periods of floods

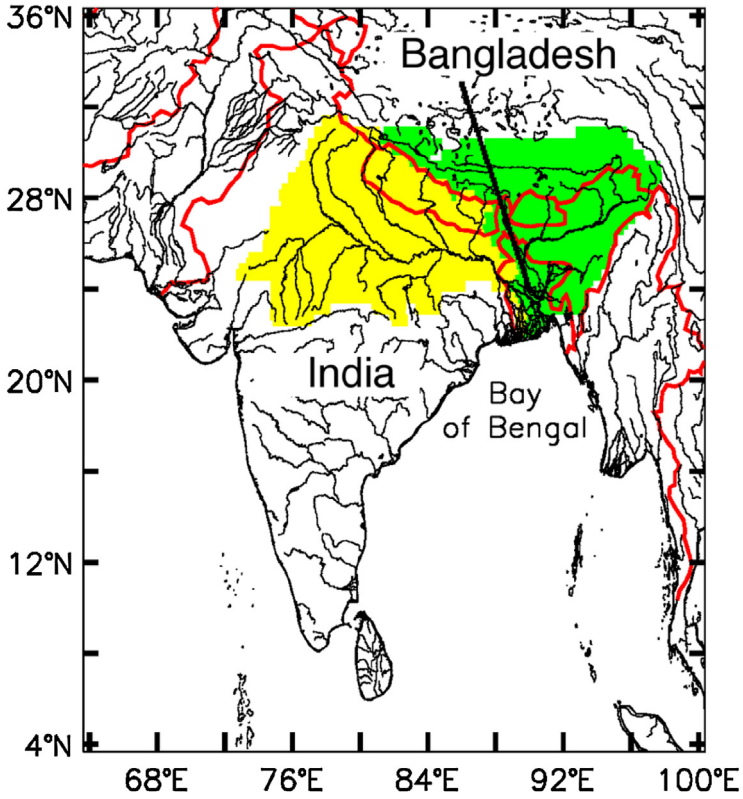

Fig. 1. Ganges and Brahmaputra River Basin, with the respective catchment areas shown in yellow (Ganges) and green (Brahmaputra). The red lines show the political borders. (For interpretation of the references to color in this figure legend, the reader is referred to the web version of the article.)

or droughts and water management is problematic due to the growing demands for a continually increasing population and needs for the agriculture and industrial sectors (Gain and Wada, 2014; Asada and Matsumoto, 2009). Facing huge development pressures, the supply of clean and uncontaminated freshwater has fallen far short of demand and part of the ISC is now facing acute shortages of drinking and agricultural water supply (Hoekstra et al., 2012; Babel and Wahid, 2008).

In Bangladesh, for instance, the intensive use and over-abstraction of groundwater for dry-season irrigation and city water supply has led to a rapid decline of groundwater tables in many parts of the country (Shamsudduha and Uddin, 2007; Shamsudduha et al., 2009, 2011; Konikow and Kendy, 2005; Hoque et al., 2007). As current groundwater withdrawal possibly exceeds the potential groundwater recharge, reduction in long-term groundwater storage, referred to as "groundwater depletion", have recently been reported in Northern India and Bangladesh (Rodell et al., 2009; Tiwari et al., 2009; Shamsudduha et al., 2012).

Consequently, there is now a widespread recognition of the need for better monitoring of terrestrial freshwater dynamics; this would enable us to properly quantify their impacts and links to climate variability and anthropogenic pressure.

Until recently, our knowledge of the spatio-temporal variations of continental waters relied upon sparse *in situ* observations, global land surface models and global-regional hydrological models. But *in situ* gauge observations provide limited information about large spatial dynamics of terrestrial waters and their public access for transboundary rivers, such as GB, is restricted by government agencies (Papa et al., 2010b, 2012a). The lack of spatial–temporal observations of freshwater storage at large, basin scale limits our ability to monitor and forecast the available supply of freshwater over the

entire GB basin (Alsdorf et al., 2007; Decharme et al., 2008, 2012; Yamazaki et al., 2011; Getirana et al., 2012).

In this context, remote sensing techniques have been very useful to hydrology investigations especially over the last twenty years and with the advent of monitoring hydrology from space (Alsdorf et al., 2007; Papa et al., 2013; Frappart et al., 2006; Calmant et al., 2008; Prigent et al., 2007, among others). The concept of measuring the hydraulics of inland water bodies from space was first brought forth in the late 1990s based on the successes of the Topex-POSEIDON (T-P) radar altimetry mission that provided a systematic monitoring of water levels of lakes (Birkett, 1995; Crétaux et al., 2005) large rivers (Birkett et al., 2002) and floodplains (Frappart et al., 2005). Multi-satellite remote sensing techniques also provide important information on land surface waters, such as the spatial and temporal variations in surface water extent at the global scale (*e.g.*, Papa et al., 2006, 2008a, 2010a; Prigent et al., 2001, 2007, 2012).

Since 2002, the Gravity Recovery And Climate Experiment (GRACE) provides, for the first time, precise measurements of spatio-temporal variations in total terrestrial water storage or TWS (the sum of ground water, soil water, surface water and snow pack) (Ramillien et al., 2005; Tapley et al., 2004) at seasonal and basin scales. Several studies have estimated groundwater storage change (GWS) from GRACE-derived TWS change after deducting the contribution of changes in the other water storage compartment, including soil moisture storage (SMS), surface water storage (SWS) and ice and snow storage (ISS). Indeed, over a period of time (t), the change in GWS can be obtained from the following decomposition of change in TWS:

$$\Delta GWS_t = \Delta TWS_t - \Delta SWS_t - \Delta SMS_t - \Delta ISS_t \quad (1)$$

Accurate partitioning of GRACE-derived ΔTWS into the different water storage contributions is therefore critical in quantifying ΔGWS. Several approaches using auxiliary information on the other components of TWS, from either *in situ* observations or land-surface models are used to produce a time series of groundwater storage anomalies in northern India (Rodell et al., 2009), in the Indo-Gangetic Plains (Tiwari et al., 2009) and in Bangladesh (Shamsudduha et al., 2012).

However, as the contribution of SWS to TWS can be substantial, sometimes up to 50% especially in humid environments and in monsoon dominated river basins (Papa et al., 2013; Shamsudduha et al., 2012; Frappart et al., 2008, 2011, 2012; Han et al., 2009; Kim et al., 2009), the use of global-scale land surface models or sparse *in situ* measurements is not sufficient to accurately quantify SWS changes in order to estimate GWS from GRACE data.

Recently, some efforts have been undertaken to quantify the surface freshwater storage and its variations at seasonal to interannual time scales, using satellite observations. The approach combines surface water extent observations from a multi-satellite technique (Papa et al., 2010a; Prigent et al., 2007, 2012; the Global Inundation Extent from Multi-Satellite called hereafter (GIEMS)) and radar altimeter-derived height variation of rivers, wetlands and flood inundations (Frappart et al., 2006). It was first developed and applied over the Rio Negro, a sub-basin of the Amazon (Frappart et al., 2008, 2011), and also tested over a boreal environment in the Ob River basin (Frappart et al., 2010). Using continuous water level observations derived from the Environmental Satellite (ENVISAT) radar altimeter (Santos et al., 2012) between 2003 and 2007, Frappart et al. (2012) provides for the first time monthly variations of SWS for the entire Amazon basin highlighting the exceptional drought of 2005. The combination of GIEMS and altimeter observations has thus proved to be a new powerful and reliable tool for monitoring large-scale surface freshwater storage dynamics and for understanding basin-scale hydrology.

In this work, we propose to further develop this observation-based technique to estimate SWS variations in rivers, floodplains, lakes and wetlands of the GB basin for the period 2003–2007, and together with GRACE measurements, to quantify the "subsurface water storage" change (SSWS, *i.e.*, the sum of GWS and SMS changes).

Section 2 presents the datasets used in this study. In Section 3, we discuss the methodology for deriving SWS from a combination of multi-satellite observations. In Section 4, the results are presented and discussed over the 2003–2007 period. An evaluation is performed comparing the new estimates

with other external datasets such as GRACE-derived TWS, *in situ* river discharge observations and precipitation. Finally, conclusions and perspectives are presented in Section 5.

2. Dataset and evaluation

2.1. Multi-satellite-based surface water extent dynamic (GIEMS)

The complete methodology that captures the extent of episodic and seasonal inundation, wetlands, rivers, lakes and irrigated agriculture, at the global scale, is described in detail in Prigent et al. (2001, 2007, 2012) and Papa et al. (2006, 2010a). The technique, which we summarize here, uses a complementary suite of satellite observations covering a large wavelength range: 1) Advanced Very High Resolution Radiometer (AVHRR) visible (0.58–0.68 μm) and near-infrared (0.73–1.1 μm) reflectances and the derived Normalized Difference Vegetation Index (NDVI); (2) passive microwave emissivities between 19 and 85 GHz. These are estimated from the Special Sensor Microwave/Imager (SSM/I) observations by removing the contributions of the atmosphere (water vapor, clouds, rain) and the modulation by the surface temperature (Prigent et al., 1997, 2006). The technique uses ancillary data from the International Satellite Cloud Climatology Project (ISCCP) (Rossow and Schiffer, 1999) and the National Centers for Environment Prediction (NCEP) reanalysis (Kalnay et al., 1996); (3) backscatter at 5.25 GHz from the European Remote Sensing (ERS) satellite scatterometer.

Observations are averaged over each month and mapped to an equal area grid of 0.25° resolution at the equator (each pixel equals 773 km^2) (Prigent et al., 2001, 2006). An unsupervised classification of the three sources of satellite data is performed and the pixels with satellite signatures likely related to inundation are retained. For each inundated pixel, the monthly fractional coverage by open water is obtained using the passive microwave signal and a linear mixture model with end-members calibrated with scatterometer observations to account for the effects of vegetation cover (Prigent et al., 2001, 2007). As the microwave measurements are also sensitive to the snow cover, snow and ice masks are used to filter the results and avoid any confusion with snow-covered pixels (Armstrong and Brodzik, 2005). Because the ERS scatterometer encountered serious technical problems after 2000, the processing scheme had to be adapted to extend the dataset and monthly mean climatology of ERS and NDVI-AVHRR observations are used (Papa et al., 2010a; Prigent et al., 2012). Fifteen years of global monthly water surfaces extent for the period 1993–2007 are available (Prigent et al., 2012). This dataset has been extensively (i) evaluated at the global scale (Papa et al., 2008a, 2010a; Prigent et al., 2007) and for a wide range of environments (Papa et al., 2006, 2007, 2008b; Frappart et al., 2008); and (ii) used for climatic and hydrological analyses, such as the evaluation of methane surface emissions models (Bousquet et al., 2006; Ringeval et al., 2010) and the validation of the river flooding schemes coupled with land surface models (Decharme et al., 2008, 2012; Getirana et al., 2012; Ringeval et al., 2012; Pedinotti et al., 2012).

Fig. 2 shows GIEMS characteristics over the GB basin (Fig. 2a). Fig. 2b and c shows respectively the annual mean and annual maximum extent of surface water averaged over 15 years (180 months). They exhibit very realistic distributions of major rivers (Ganges–Brahmaputra–Meghna River systems) and their tributaries and distributaries. Associated inundated areas, wetlands and the region of the Bengal delta are well delineated even in the presence of complex areas characterized by extensive flooding. The spatial distribution of GIEMS was extensively evaluated against high-resolution (100 m) SAR images in Prigent et al. (2007) and in Aires et al. (2013) over the Amazon basin leading to an overall GIEMS uncertainties of ~10% for GIEMS. Over the SIC (and especially GB), the spatial distribution of GIEMS basin was evaluated against static surface water dataset (Global Lake and Wetland Dataset, GLWD-3, (Lehner and Doell, 2004)) and other related hydrological variables (precipitation, altimeter-derived river heights, river discharge) in Papa et al. (2006) and in Prigent et al. (2012), as well as using other regional surveys representing various components of wetland and open-water distributions (Adam et al., 2010).

Seasonal and interannual variations in surface water extent and associated anomalies over the GB Basin are presented in Fig. 2d and e. The extent shows a strong seasonal cycle (Fig. 2d), with a mean annual averaged maximum of $\sim 2.1 \times 10^5$ km^2 for the period 1993–2007. It shows a substantial interannual variability especially near the maxima and the duration of the flood. The years 1994, 1998,

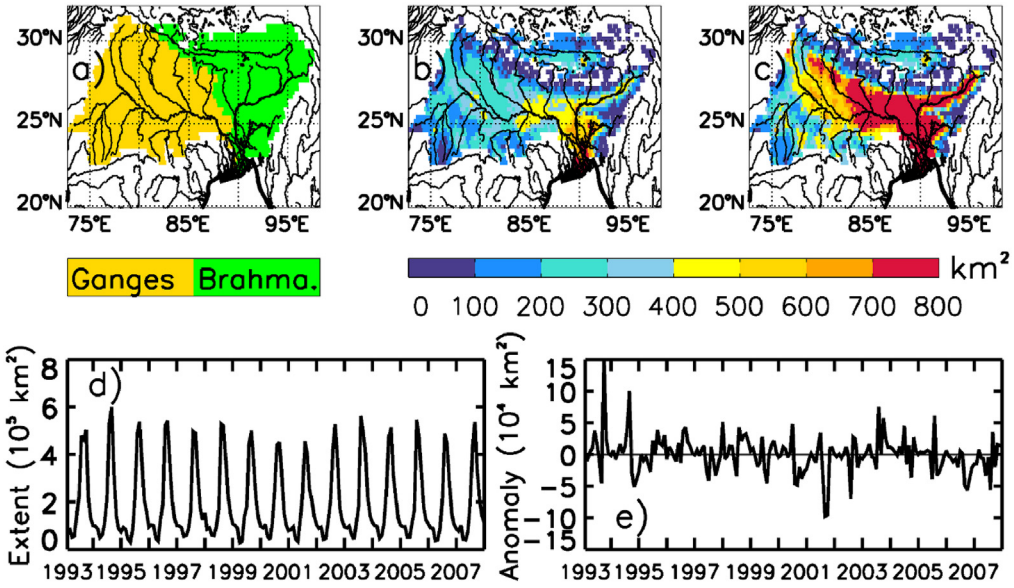

Fig. 2. The global inundation extent from multi-satellites (GIEMS, top) and anomalies (bottom) over the Ganges–Brahmaputra basin. (a) A zoom-in of Fig. 1. Spatial distribution of the (b) annual mean and (c) annual maximum surface water extent averaged over 1993–2007, for each 773 km^2 pixel. (d) Monthly mean surface water extents and (e) corresponding anomalies for 1993–2007 for the entire Ganges–Brahmaputra basin; the anomalies are constructed by subtracting the 15-year climatological monthly mean.

2003 and 2005 exhibit larger peaks (Fig. 2d and e). Drought-like conditions with negative anomalies are captured during the three consecutive years of 2000, 2001 and 2002, as well as in 2006.

Despite the fact that GIEMS is broadly able to capture the distributions and variations of surface freshwater in the GB basin, some analysis (Papa et al., 2010a; Lehner and Doell, 2004) suggested that the method might encounter difficulties in accurately discriminating between very saturated/moist soil and standing open water, especially in the delta region. This can lead to potential overestimations of actual surface water extents, especially for pixel with very high flood coverage (see the histogram sin Fig. 2d of Papa et al. (2010a)). To overcome this issue, we use here external information on flood coverage from the Dartmouth Flood Observatory database (http://floodobservatory.colorado.edu) that provides surface water extent observations derived from the MODerate-resolution Imaging Spectroradiometer (MODIS) for the period 2002–2012. In particular, we use the MODIS-derived map of maximum inundation over the GB to set a maximum threshold on GIEMS observations: when a GIEMS pixel has a value higher than the one from the MODIS-derived map of maximum inundation, the GIEMS value is replaced by the MODIS-derived maximum inundation value.

2.2. ENVISAT radar altimeter observations over the Ganges and the Brahmaputra Rivers

Radar altimeters onboard satellites are initially designed to measure the ocean surface topography by providing along-track nadir measurements of water surface elevation. For a complete description of altimetry and the construction of surface water level time series over the oceans (or ice sheets), we refer to Fu and Cazenave (2001). The technique can be summarized as follows: altimeters emit a pulse at the nadir to Earth and receive the echo back after it is reflected by the observed surface. Assuming that the pulse is propagating at the speed of light, a precise measurement of the round-trip time between the satellite and the Earth's surface gives the distance between the satellite and the surface called range *R*. However, as electromagnetic waves travel through the atmosphere, corrections related to the delayed propagation through the atmosphere or the interaction with the ionosphere

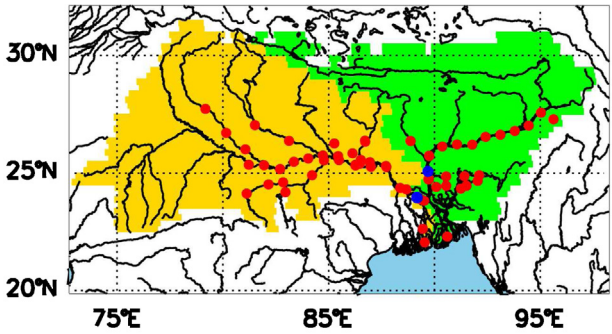

Fig. 3. The location (red circles) over the Ganges–Brahmaputra River basin of the 58 ENVISAT radar altimeter virtual stations (VS, *i.e.* where river water level variations are estimated at the intersection between the altimeter ground tracks and the river). The locations of the *in situ* discharge and river height stations (Hardinge for the Ganges and Bahadurabad for the Brahmaputra) are displayed with blue circles. The respective catchment areas are shaded as in Fig. 2a. (For interpretation of the references to color in this figure legend, the reader is referred to the web version of the article.)

need to be applied. Given that the satellite altitude Hsat, with respect to a reference ellipsoid, is known accurately by precise orbitography calculation, the height H of the observed reflector with respect to the geoid is given by:

$$\mathbf{H} = \mathbf{H}\mathrm{sat} - [\mathrm{R} + \mathbf{C}\mathrm{i} + \mathbf{C}\mathrm{d} + \mathbf{C}\mathrm{w} + \mathbf{C}\mathrm{s} + \mathbf{C}\mathrm{p}] - N, \tag{2}$$

where **C**i is the correction for delayed propagation through the ionosphere, **C**d (d for dry) and **C**w (w for wet) are corrections for delayed propagation in the atmosphere, accounting respectively for air and humidity density. **C**s and **C**p, the solid and polar tides respectively, are additional corrections applied to correct the instantaneous height disturbed by the solid Earth and polar tides into a mean, undisturbed height. N is the geoidal anomaly, substracted at the ellipsoidal height to get orthometric heights, or altitudes.

For continental water studies, radar altimeter derived water level data have long been shown to be precise enough and are now used for systematic monitoring of large rivers, lakes, wetlands and floodplains (Crétaux et al., 2005; Frappart et al., 2005; Santos et al., 2010, 2012). Over the GB river basin, Papa et al. (2010b, 2012a) used water levels measured by four altimeter satellites to infer GB river freshwater flux into the Bay of Bengal: 10-day T-P-derived Ganges and Brahmaputra river level heights from 1993 to 2001, along with 35-day ERS-2 and ENVISAT time series for the period 1995–2002 and 2002–2008 respectively and finally 10-day Jason-2 observations from 2008 onwards. Recently ENVISAT observations were used to quantify the major flood event in 2008 that affected the Kosi River, a major tributary of the Ganges (Pandey et al., 2014).

In the present study, we use ENVISAT radar altimeter observations over the GB basin in order to estimate time series of river level heights variations. As a part of the Earth Observation Program, the satellite ENVISAT was launched in March 2002 by the European Space Agency (ESA), with, among 10 other instruments, a nadir radar altimeter (RA-2 or Advanced Radar Altimeter) making high-precision dual-frequency (Ku and S bands) observations. ENVISAT is on a helio-synchronous circular orbit with an inclination of 98.5°, a 35-day repeat period and sampling the 81.5° N–81.5° S latitudinal domain. Because radar altimetry is a profiling and not an imaging technique, the ENVISAT orbit ground-track has an inter-track distance of approximately 80 km at the equator (Zelli, 1999).

Given the orbit configuration, there are several intersections between the satellites ground tracks and the Ganges and Brahmaputra rivers or their major tributaries. The intersections where water levels can be derived are termed as “virtual stations”. Fifty-eight of them were built in the GB basin using ENVISAT RA-2 measurements and their locations are shown in Fig. 3. Twenty were already available from the Hydroweb database, providing time series of water levels of large rivers, lakes and wetlands around the world (http://www.legos.obs-mip.fr/en/soa/hydrologie/hydroweb/). Following the same procedure, we constructed this dataset with 38 other virtual stations for which we derive ENVISAT time

series of water stage variations for each pass using the Virtual ALtimetry Station software (VALS, 2010, Virtual ALtimetry Station Software, Version 0.6.2, available online at www.mpl.ird.fr/hybam/outils/logiciels_test.php). VALS is a Java-based toolbox that was developed to interactively select altimetry data at the virtual stations and apply the corrections individually to satellite passes (Santos et al., 2010). The ENVISAT altimetric observations that we use come from the Centre de Topographie des Océans et de l'Hydrosphère (CTOH, http://ctoh.legos.obs-mip.fr/), a French observation service that distributes the geophysical data records provided by the space agencies with additional parameters. The VALS data processing has three steps and is described in detail in Santos et al. (2010, 2012). The first step consists of a rough selection of the region using imagery from satellite such as Google Earth or the GeoCover Landsat Thematic Mapper orthorectified mosaics available from the MrSID Image Server at https://zulu.ssc.nasa.gov/mrsid/mrsid.pl). The second step consists of refining the selection in a cross-sectional view. The third step consists of the computation of master points per pass. Following the conclusions of Frappart et al. (2006), the median value instead of the mean value is computed for each pass using the data subset selected in the second step. In order to estimate the range R (Eq. (2)), several tracker algorithms can be used to best fit the highly variable time distribution of the echo energy bounced back by the very different types of surfaces in the satellite field of view. Comparing the performances of several existing algorithms (OCEAN, Ice-1, Ice-2. . .) for continental hydrology, Frappart et al. (2006), and more recently Santos et al. (2010) concluded that the Ice-1 algorithm, primarily designed for ice sheets, provided the most robust estimated water stages on rivers and lakes. Therefore, here we use the range values calculated by the Ice-1 retracking algorithm. Finally, river height water levels are referenced to the Earth Gravitational Model EGM2008 (Pavlis et al., 2008) with respect to WGS 84 reference (The World Geodetic System 1984, http://earth-info.nga.mil/GandG/wgs84/). It is important to note that, in terms of single river level height measurements, there are several other factors, beside the choice of a certain tracker to retrieve the altimetric range or the river width, that could introduce uncertainties in the height measurements: for instance, the precision of the estimated satellite orbit or the uncertainties in datasets used to correct atmospheric contributions can also have a non-negligible impact. However, uncertainties/errors due to these factors will not be evaluated nor discussed in this paper.

The time series at each location is available for the period August 2002 to October 2010, date when the ENVISAT satellite was placed on another orbit. Note that for 8 virtual stations located on ENVISAT descending tracks, the time series present significant gaps for the cycles 31–55 (from 05/10/2004 to 26/02/2007). This corresponds to cycles when ESA chose the northern part of the ISC region to systematically perform the control operations on the satellite. During these operations, the ENVISAT altimeter was not operating. For these virtual stations, we replace the missing observations with the monthly average estimated at the virtual station over the period October 2002 to October 2010.

2.3. Ancillary data

2.3.1. GRACE data

The Gravity Recovery And Climate Experiment (GRACE) mission, launched in March 2002, provides measurements of the spatio-temporal changes in Earth's gravity field. At basin scale, GRACE data can be used to derive the monthly changes of the total land water storage (Ramillien et al., 2005; Landerer and Swenson, 2012) with an accuracy of ~1.5 cm of equivalent water thickness when averaged over surfaces of a few hundred square-kilometers. In this study, we use monthly GRACE solutions from the Geo Forschung Zentrum (GFZ), the University of Texas Center for Space Research (UTCSR) and the Jet Propulsion Laboratory (JPL) from February 2003 (data are missing for January 2003) to December 2007 in order to analyze the time variations of the water mass changes in the GB basin. Unfortunately, the GRACE solutions suffer from the presence of an unrealistic high frequency noise corresponding to north-south striping that is caused by orbit resonance during the Stokes coefficients determination and aliasing of poorly modeled short-term phenomena. To attenuate the noise in the Level-2 GRACE solutions, we used the global solutions post-processing by an Independent Component Analysis (ICA) approach based on the combination of GFZ/UTCSR/JPL solutions of the same monthly period to isolate statistically independent components of the observed gravity field, and mainly the continental water

storage contribution (Frappart et al., 2010b, 2011b). These data will be soon available at: http://bgi.obs-mip.fr/

2.3.2. Precipitation estimates from TRMM 3B43

We used the Tropical Rainfall Measuring Mission (TRMM) 3B43 v7 product which is a combination of monthly rainfall at a spatial resolution of 0.25° and currently available from January 1998 to December 2013. This dataset is obtained by combining satellite information from the passive TRMM Microwave Imager (TMI) and Precipitation Radar (PR) onboard the Tropical Rainfall Measuring Mission (TRMM), a Japan-U.S. satellite launched in November 1997, the Visible and Infrared Scanner (VIRS) onboard the Special Sensor Microwave Imager (SSM/I) and rain gauge observations. The dataset results from the coupling of the TRMM 3B42-adjusted merged infrared precipitation with the monthly accumulated Climate Assessment Monitoring System or Global Precipitation Climatology Center Rain Gauge analyses (Huffmann et al., 2007). It is available on the Goddard Earth Sciences Data and Information Services Center (GES DISC) website: http://daac.gscf.nasa.gov

2.3.3. Ganges–Brahmaputra in situ river heights and altimeter-derived river discharge

We use hydrological observations over the Ganges and Brahmaputra Rivers in Bangladesh monitored by the Bangladesh Water Development Board (BWDB) [http://www.bwdb.gov.bd/]. These data, including *in situ* river level and discharge, are collected at the two basin outlet stations before the confluence of these two rivers, as shown in Fig. 3: the Hardinge Bridge station (24.07° N; 89.03° E) for the Ganges and the Bahadurabad station (25.15° N; 89.70° E) for the Brahmaputra (Papa et al., 2010b, 2012a). In order to evaluate radar altimeter time series, we will use *in situ* river height measurements comprising of 858 infrequent measurements made at Hardinge station for the Ganges from May 2006 to August 2011 and 102 infrequent measurements made at Bahadurabad station for the Brahmaputra from January 2008 to August 2011. This is also discussed further in Section 2.4.

Along with the *in situ* river level measurements, the results regarding the surface water storage are evaluated against the total discharge at the Ganges–Brahmaputra mouths derived from satellite altimeter as in Papa et al. (2010b, 2012a).

2.4. Evaluation of ENVISAT radar altimetry over the Ganges–Brahmaputra

The uncertainty associated with the altimeter-derived water level height of large rivers ranges from 5–25 cm for high water season to 12–40 cm during low water season (Frappart et al., 2006; Santos et al., 2012). In order to evaluate ENVISAT performances over the Ganges and Brahmaputra, we select the nearest virtual stations to the Hardinge and Bahadurabad gauging stations (Fig. 3). The virtual station on the Ganges (23.82° N; 89.52° E, on the ENVISAT track 337) is located ~40 km downstream of Hardinge and the one on the Brahmaputra (25.72° N; 89.76° E, on the ENVISAT track 795) is located ~50 km upstream of Bahadurabad. At these locations, the river width for low/high water stages is 3/6 km for the Ganges and 4/10 km for the Brahmaputra.

Fig. 4 shows the ENVISAT-derived times series of river level height at Hardinge and Bahadurabad (estimated in Section 2.2) and the comparison with the *in situ* river level measurements at each station. Note that these two datasets are independent. Since altimeter-derived water level heights are expressed with respect to a geoid model, there is no common height reference when compared to *in situ* water level heights, resulting in a natural difference in absolute values. A large seasonal cycle is observed with annual height variations exceeding 8 m for both rivers. For the period of common availability, times series (every 35 days for the altimeter-derived observations) show a very good agreement (Fig. 4a and c) and have a similar behavior in the peak-to-peak height variations. Over the Ganges, from 2006 to 2010, there are 38 dates where measurements are simultaneously available (*i.e.*, plus or minus two day apart). Similarly, for the Brahmaputra, there are 29 measurements simultaneously available for the ENVISAT-derived and the *in situ* height observations. Fig. 4b and d show the relationship between the satellite-derived river height and the *in situ* observations, confirming the good agreement between the two data sets with a correlation of 0.98 (p-value (hereafter, p) <0.01) and 0.99 ($p < 0.01$) for the Ganges and the Brahmaputra, respectively. We estimated the standard error to be of ~0.36 m at Hardinge and ~0.29 m at Bahadurabad, which is typically in the range of accuracy

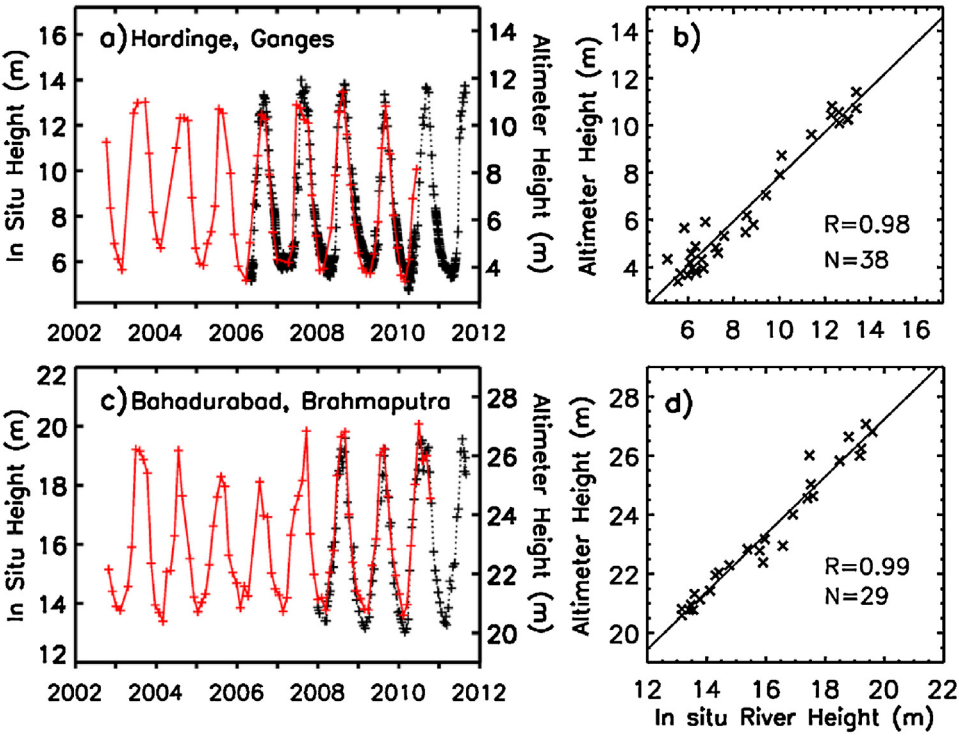

Fig. 4. Comparison of *in situ* river level height measurements (black line and + symbols; 2006–2011) of (a and b) Ganges (Hardinge) and (c and d) Brahmaputra (Bahadurabad) with 35-day ENVISAT altimeter-derived river level height (red line and + symbols; 2002–2010) at virtual stations. The virtual stations on the two rivers are ~45 km downstream of Hardinge and ~50 km upstream of Bahadurabad. The best-fit correlation coefficients (R) and sample size (N) are shown in panels (c) and (d). (For interpretation of the references to color in this figure legend, the reader is referred to the web version of the article.)

of altimetric observations over large rivers (0.1–0.2 m for instance over the Amazon (Frappart et al., 2006; Birkett et al., 2002)). These results are similar to the 0.28 m (resp. 0.19 m) found using Jaons-2 over the Ganges (resp. the Brahmaputra) in Papa et al. (2012a).

Note that this accuracy strongly depends, among other factors, on the width and morphology of river channels and their banks. In general, the accuracy is reduced over narrower rivers and/or in presence of vegetation. For instance, at the virtual stations, the width of the river channel is always larger in the Brahmaputra River than the Ganges, River, which might explain in part the marginally better accuracy of the river level measurements over the Brahmaputra River than over the Ganges River. Nevertheless, the good match between ENVISAT-derived water level height and *in situ* observations at Hardinge and Bahadurabad gives confidence for using radar altimeter-derived time series over the GB basin.

3. Methodology to estimate the surface water storage

The method used to estimate surface freshwater storage consists of the combination of the surface water extent from GIEMS (Section 2.1) with altimeter-derived water level heights estimated at 58 virtual stations (Section 2.3.1). Here we use both dataset during their coincident years of availability, the period of 2003–2007. The two-step methodology is described in details in Frappart et al. (2011, 2012) and is briefly summarized below.

3.1. Monthly water level maps

Monthly maps of water level over the GB River Basin are generated by combining the observations from GIEMS and ENVISAT RA-2 derived water levels. Following Frappart et al. (2008, 2011), water levels for a given month are linearly interpolated over the GIEMS pixels which are estimated as inundated. Each monthly map of surface water levels has a spatial resolution of 0.25° and the elevation of each pixel is given with reference to a map of minimum water levels estimated for the entire observation period (2003–2007) using a hypsometric approach (see Figure S1 from Frappart et al. (2012) and Papa et al. (2013)). This approach helps to take into account elevation differences in each cell area, for instance, the difference in elevation between the river level and the floodplain. For each inundated pixel P of coordinates (λ_i,φ_i), the minimum elevation h_{min} during the observation period ΔT for a percentage of inundation α from GIEMS is given as:

$$h_{\min}(\lambda_i, \varphi_i, \alpha, \Delta T) = \min\left(h(\lambda_i, \varphi_i, t)\right)_{P(\lambda_i,\varphi_i,t)\leq\alpha; t\in\Delta T} \tag{3}$$

where α varies between 0 and 100 and t is a monthly observation during ΔT.

The minimum elevation H_{min} for a pixel of coordinates (λ_i,φ_i) during the observation period ΔT is hence:

$$H_{\min}(\lambda_i, \varphi_i, \Delta T) = \frac{1}{100}\sum_{\alpha=0}^{100} h_{\min}(\lambda_i, \varphi_i, \alpha, \Delta T)\Delta\alpha \tag{4}$$

where $\Delta\alpha$ is the increment in percentage of surface water extent (a step of 1% was chosen here).

Fig. 5 shows the seasonal evolution of water levels in the GB basin for the period May 2007 to October 2007 covering a full monsoon period. The maps exhibit very realistic spatial patterns over the season with increasing water levels in June-July (up to 4–5 m) to reach their maximum values in the lower part of the basin in August-September (up to 7–8 meters), particularly in the lower reaches of the Ganges and Brahmaputra Rivers, similar to what is observed in the *in situ* gauge records at Hardinge and Bahadurabad. From October, the water levels start to decline, responding to the end of monsoon season.

3.2. Monthly GB time series of surface water volume variations

Following (Frappart et al., 2011, 2012), the time variations of surface water volume at the basin scale, are computed as

$$V_{SW}(t) = R_e^2 \sum_{j\in S} P(\lambda_j, \varphi_j, t)\left(h(\lambda_j, \varphi_j, t) - h_{\min}(\lambda_j, \varphi_j)\right)\cos(\varphi_j)\Delta\lambda\Delta\varphi \tag{5}$$

where V_{SW} is the volume of surface water, R_e the radius of the Earth (6378 km), $P(\lambda_j,\varphi_j,t)$, $h(\lambda_j,\varphi_j,t)$, $h_{min}(\lambda_j,\varphi_j)$ are respectively the percentage of inundation, the water level at time t, and the minimum of water level at the pixel (λ_j,φ_j); $\Delta\lambda$ and $\Delta\varphi$ are respectively the grid steps in longitude and latitude. The minimum of water level is estimated through a hypsometric approach relating the percentage of inundation of a pixel to its elevation. Monthly surface freshwater storage and their variations are estimated for the period of 2003–2007. Following Frappart et al. (2008, 2011), the maximum error on the volume variation is estimated as

$$\Delta V_{SW,\max} \leq \Delta S_{\max}\delta h_{\max} + S_{\max}\Delta(\delta h_{\max}) \tag{6}$$

where $\Delta V_{sw,\max}$ is the maximum error on the water monthly volume anomaly, $S_{\max}$ is the maximum monthly flooded surface, $\delta h_{\max}$ is the maximum water level variation between two consecutive months, $\Delta S_{\max}$ is the maximum error for the flooded surface, and $\Delta(\delta h_{\max})$ is the maximum error for the water level between two consecutive months.

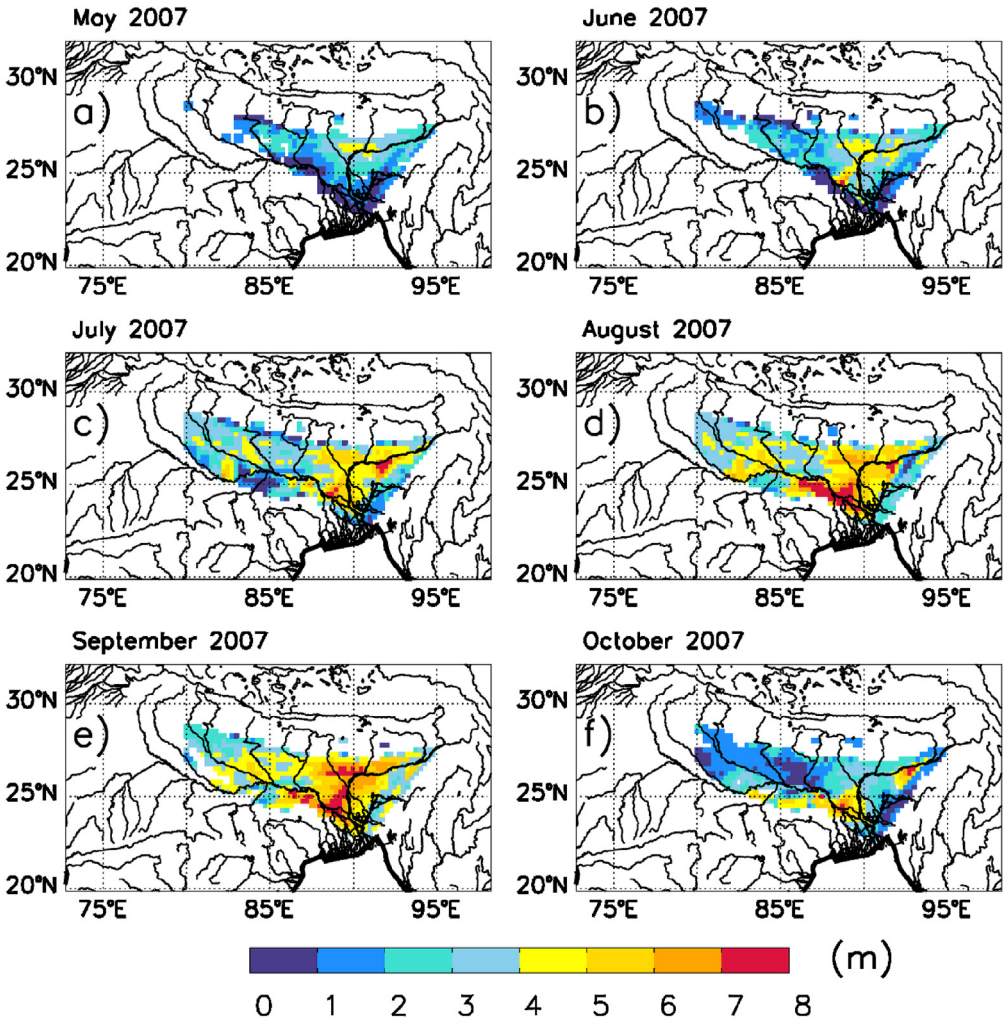

Fig. 5. Seasonal evolution (May through October 2007) of the spatial distribution of water level heights in the Ganges–Brahmaputra River basin from a combination of GIEMS and ENVISAT satellite observations.

3.3. *Monthly GB time series of rainfall and TWS volume variations*

Accordingly, the time variations of volume of rainfall from TRMM and *TWS* anomalies from Level-2 GRACE solutions filtered using an Independent Component Analysis (ICA) approach are computed following Ramillien et al. (2005):

$$\Delta V_{TWS}(t) = R_e^2 \sum_{j \in S} \left\{ \begin{matrix} P \\ \Delta h_{tot} \end{matrix} \right\} (\lambda_j, \varphi_j, t) \cos(\varphi_j) \Delta\lambda \Delta\varphi \tag{7}$$

where $P(\lambda_j,\varphi_j,t)$ and $h_{tot}(\lambda_j,\varphi_j,t)$ are the rainfall and the anomaly of *TWS* at time t of the pixel of coordinates (λ_j,φ_j) respectively.

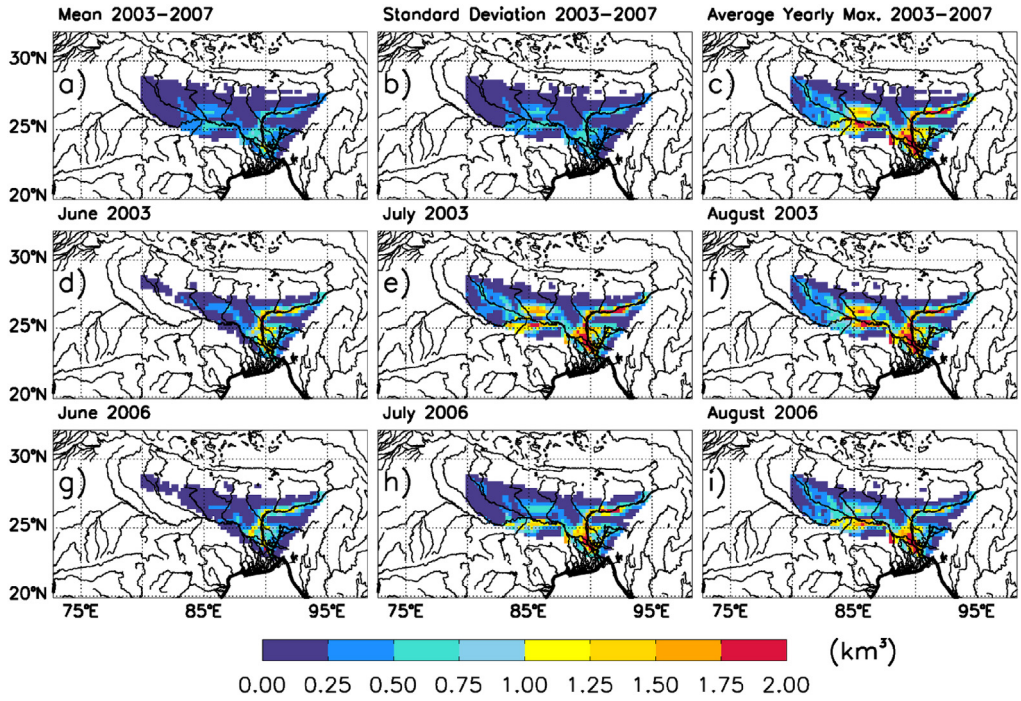

Fig. 6. Maps of Ganges–Brahmaputra surface freshwater volume variations from 2003 to 2007 and evolution for two contrasted years. (a and b) Annual mean and standard deviation (STD) of surface water volume averaged over 2003–2007, for each pixel of 0.25° × 0.25°. (c) Annual maximum surface water volume averaged over 2003–2007. (d–f) Surface water volume evolution during the summers (JJA) 2003. (g–i) Surface water volume evolution during the summers (JJA) 2006.

4. Results, evaluation and discussion

Fig. 6 shows the spatial distribution (annual mean, standard deviation, and mean annual maximum) of SWS for the entire GB basin. In parallel, Fig. 7 exhibits the temporal variations over the period of 2003–2007 (Fig. 7a, c and e) and the seasonal cycle (averaged over 2003–2007, Fig. 7b, d and f) of the surface water volume aggregated for entire GB basin, and only the Ganges and Brahmaputra Basins. These time series are compared with GRACE-derived TWS over the same period and same geographical locations mentioned above.

In terms of spatial distribution, Fig. 6 shows realistic structures with larger surface water volume and changes observed along the main stems and major tributaries/distributaries of both rivers. Following the spatial distribution observed in GIEMS estimates (Fig. 2), both floodplains associated with the river channels in the GB Basin and delta plains in southern Bangladesh are well delineated. On average, Fig. 6a and b show SWS variations along the main stems of less than ~1 km^3. Fig. 6c shows that SWS can reach up to more than 2 km^3 during the monsoon period with high SWS at pixel level in the main channels of the Ganges and Brahmaputra. Fig. 6 also shows that during the summer season (June–July–August), the evolution of SWS greatly varies for two hydrological contrasted years, 2003 (Fig. 6d–f) and 2006 (Fig. 6g–i). The seasonal evolution shows that SWS initially increases in the main channel of the Brahmaputra River in June, followed by an increase in SWS in July in the Gangetic floodplains, along main channel of the Ganges and at the confluence of the GB rivers. The maximum SWS is reached in August. Higher SWS is observed in 2003 compared to 2006, revealing a rather strong year-to-year variability. In terms of temporal variation, as expected, a strong seasonal cycle is evident (Fig. 7), for both rivers and the entire GB basin. For GB basin, the mean annual amplitude of SWS is of ~410 km^3 (Fig. 7a and b). This amounts to ~39% of the total volume of water that flows out the GB

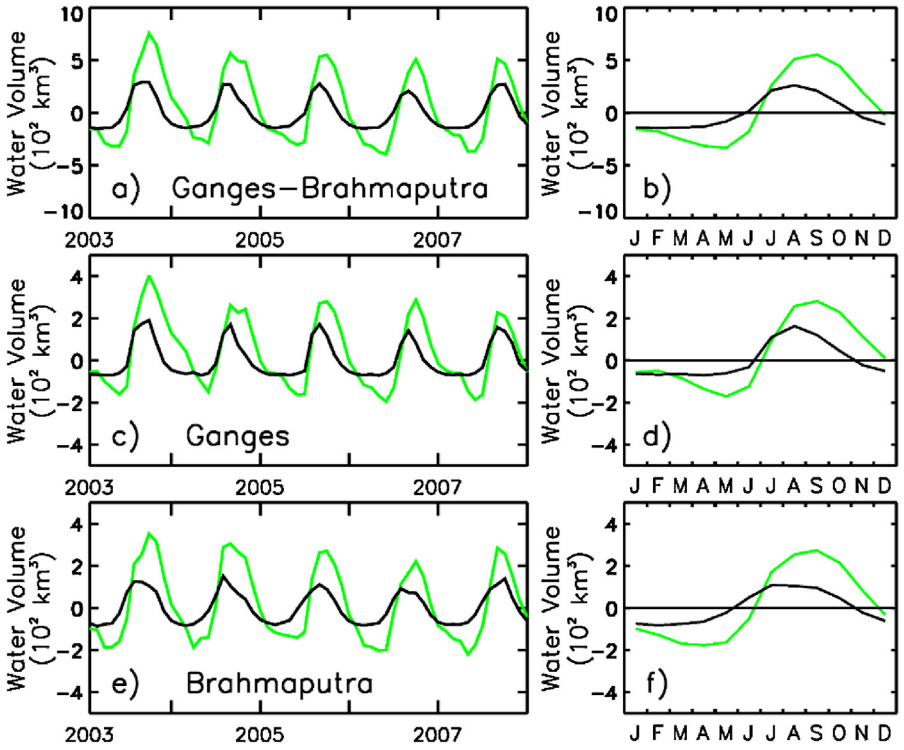

Fig. 7. Comparison of the monthly (a, c and e) mean and (d–f) climatology (2003–2007) of surface freshwater water volume (black) with the GRACE-derived total water storage (green) for the entire Ganges–Brahmaputra Basin and the two rivers individually. (For interpretation of the references to color in this figure legend, the reader is referred to the web version of the article.)

basin into the Bay of Bengal annually (Papa et al., 2012a; Dai et al., 2009). Using (6), we estimated the maximum error for the volume change in the G–B basin with the following values:

$$S_{max} = 191,000\,km^2;$$

δh_{max} = 1 m, mean maximum water level change between two consecutive months during the study period over the whole area;

ΔS_{max} = 10% from Prigent et al. (2007) of 191,000 km^2;

$\Delta(\delta h_{max})$ = 0.4 m, maximum dispersion of the altimeter measurements over the whole area. For GB, we obtained a maximum error of ~96 km^3 for a mean annual variation of 410 km^3, *i.e.*, an error of ~24%. This is of the same order of magnitude as the maximum error (23%) found over the Rio Negro in Frappart et al. (2008, 2011).

SWS gradually builds in June and reaches a maximum value is observed in August, one month ahead of the annual peak in GRACE-derived TWS, and SWS starts to decrease from September to reach a minimum value in January–February, three months before GRACE-derived TWS minimum is recorded in May. This delay can be explained by the exchange of water from the surface reservoir to the sub-surface/groundwater reservoir and by the slower sub-surface/groundwater flow in comparison to the surface water movement, causing this 1-to-3-month delay in the annual cycle and in the peaks timing. A similar behavior is observed for the Ganges and Brahmaputra basins separately. Specifically, the SWS annual amplitude is ~300 km^3 for the Ganges whereas it is slightly lower for the Brahmaputra, 250 km^3, with a peak value observed in July, two month ahead of the GRACE-derived TWS peak in September. Fig. 7b also shows that the annual variations in surface water reservoir represents about

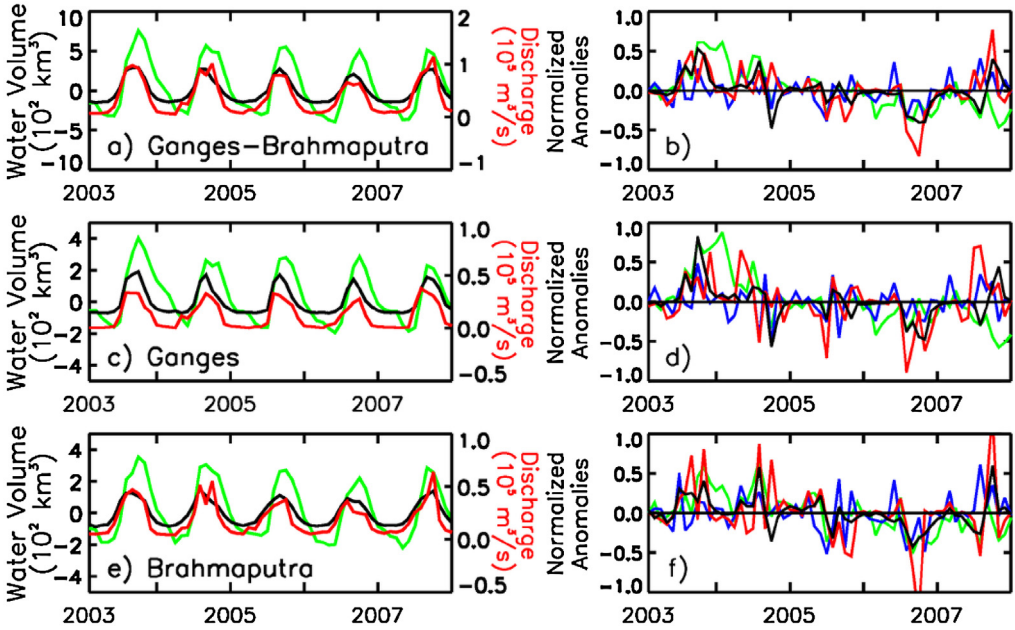

Fig. 8. (a, c and e) Correspondence between the satellite-derived monthly mean surface water storage (black), altimeter-derived river discharge (red) and GRACE-based total water storage (green) for the entire Ganges–Brahmaputra Basin and for the two rivers individually. (b, d and f) Corresponding anomalies of the mean quantities shown in (a, c and e), along with the anomalies of TRMM-based (3B43) precipitation (blue). The anomalies shown are constructed by removing the 5-year (2003–2007) climatology and normalizing by the corresponding standard deviation. (For interpretation of the references to color in this figure legend, the reader is referred to the web version of the article.)

~45% of the TWS variations as measured by GRACE. The seasonal SWS variations represent ~51% and ~41% of the GRACE-derived TWS variations in the Ganges and the Brahmaputra basin respectively.

The new estimates of surface water storage also show a substantial interannual variability at basin scale (despites the short 5-year record), especially in terms of annual maximum. For instance, the year 2003 exhibits a larger summer peak than in 2006 for all three cases. The correlation coefficients between surface water storage and GRACE-derived TWS are high with $R = 0.95$ (60 months, p-value < 0.01) and a lag-time of 1 month for the GB basin ($R = 0.91$ with a lag-time of 1 month for the Ganges basin and $R = 0.96$ with a lag-time of 1 month for the Brahmaputra basin).

Given the absence of other independent, large-scale, multiyear SWS estimates over the GB basin, the seasonal and interannual variability of our results over 2003–2007 are evaluated by comparison with related hydrological variables (Fig. 8): (i) satellite altimeter-derived river discharge measured at Hardinge and Bahadurabad (see Fig. 3 for their locations) and at the GB river mouths (Papa et al., 2010b, 2012a); (ii) basin-scale estimates of precipitation from TRMM (Huffmann et al., 2007); (iii) and variations of GRACE-derived TWS.

Fig. 8a shows that the time series of the river discharge is closely linked to the total amount of SWS in the entire basins, with a high maximum lagged correlation ($R > 0.90$). Furthermore, the lagged correlation between the SWS and basin-averaged precipitation also high (>0.8), with rain leading the SWS changes by 1 month. The normalized deseasonalized anomalies (computed by subtracting the 5-year mean monthly value from the monthly time series) also show good agreement in the temporal patterns between the four variables (Fig. 8b, d and f).

Fig. 8 also shows wetter and dryer events associated with natural hydrological variability. A good agreement over the two river basins is observed among all variables for the positive anomalies of 2003 and 2007 and the negative anomalies of 2004 and especially 2006. Droughts and floods events can affect a large part of the GB river basins with large impacts and consequences on population

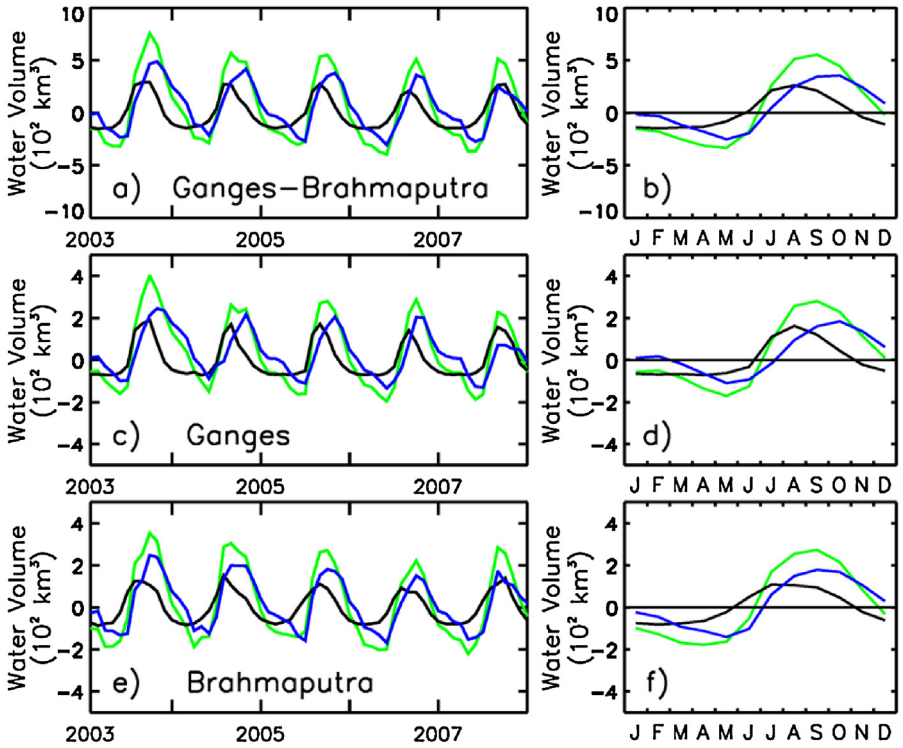

Fig. 9. Comparison of the monthly (a, c and e) total water storage (green), surface freshwater storage (black) mean and the resulting subsurface water storage (blue) variations for the entire Ganges–Brahmaputra Basin and the two rivers individually. (b, d and f) Corresponding seasonal cycles (based on 2003–2007). (For interpretation of the references to color in this figure legend, the reader is referred to the web version of the article.)

and human activities, as well as on the regional climate and biogeochemical and carbon cycles. Our new dataset now offers the opportunity to study the signatures of such droughts on the dynamics of SWS. For instance, we estimate that the amount of surface water stored in the entire GB basin during July–September 2006 was about ~60 km^3 that is ~30% below for the July–September months compared to 2003–2007 average, with a maximum deficit of ~35% in SWS for the Brahmaputra River basin.

Disaggregation of GRACE-derived TWS into satellite-derived Sub-Surface Water Storage variations (SSWS) is carried out following equation (1) and using our new SWS estimates. SSWS is defined as the sum of GWS and SMS changes. We assume that changes in freshwater storage derived from ice and snow (ISS) are negligible and hence not considered here. The choice of estimating the sole sub-surface water storage variations instead of disaggregating this term into GWS and SMS changes is driven by the poor quality and the large uncertainties associated with existing satellite-derived (AMSR-E, SMOS, representative of the very first cm below the surface) and land-surface model outputs of soil moisture over the GB basin. Over Bangladesh, for instance, Shamsudduha et al. (2012) reported large differences in the SMS annual amplitudes in three commonly used land-surface models (CLM, NOAH, VIC) with differences up to 300% among the datasets.

Monthly estimates of water storage in the three different hydrological reservoirs are computed for 5 years (2003–2007) and are shown in Fig. 9 (the black curves and green curves are identical to the ones in Fig. 7). In agreement with the results of TWS and SWS changes, SSWS also shows a strong seasonal cycle, for the entire GB basin (Fig. 9a), and for each of the rivers (Fig. 9c and e). For the GB basin, the mean annual amplitude of SSWS is ~550 km^3 (Fig. 9a and b) with a peak amplitude in October.

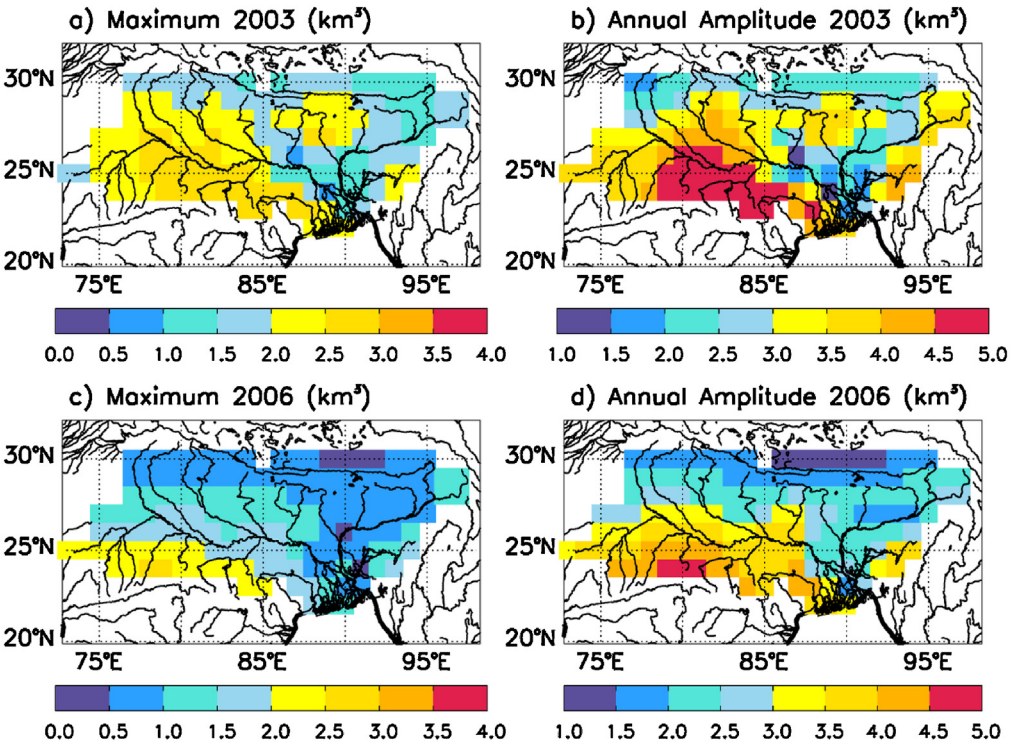

Fig. 10. Spatial distribution of the Ganges–Brahmaputra sub-surface (soil moisture + groundwater) water volume anomalies for two contrasting years, 2003 (wet) an 2006 (dry). (a) Maximum anomaly for the year 2003, for each pixel of $1^\circ \times 1^\circ$. (b) Annual amplitude (the difference between the annual maximum and minimum values) for the year 2003. (c and d) Same as (a and b) for the year 2006.

A similar pattern is observed for the Ganges and Brahmaputra basins, with an annual amplitude of ~290 km^3 for the Ganges River (peak in October) and ~320 km^3 for the Brahmaputra river (peak in August). However, because of the lack of independent, basin-scale and varying estimates of SSWS over the region, the seasonality and variability of our results cannot be thoroughly evaluated. Our results are of the same order of magnitude as some crude estimates of the total replenishable groundwater resources in the Ganges River basin estimated to be around ~180 km^3/year (source: http://www.nih.ernet.in/rbis/rbis.htm from the National Institute of Hydrology, Roorkee, India).

Finally, Fig. 10 shows a spatial distribution of Ganges–Brahmaputra SSWS anomalies for two contrasted years, 2003 (wet) and 2006 (dry), during the period 2003–2007. During 2003, maximum anomaly of SSWS (Fig. 10a) can reach up to 3 km^3 in the Ganges River basin, with an annual amplitude (Fig. 10b) more than 5–6 km^3, especially in the southern west part of the basin. On the contrary, 2006, a dryer year, shows lower maximum anomalies of SSWS (Fig. 10c, below 2 km^3) and smaller annual amplitude reaching at most 4 km^3 (Fig. 10d).

When reliable information on SMS changes at basin-scale becomes available, our new estimates of SWS can be applied to disaggregate SSMS anomalies to derive GWS changes over the GB Basin.

5. Conclusion and perspectives

This study presents an observation-based dataset that quantifies basin the monthly distribution and variation of surface freshwater storage for the entire Ganges–Brahmaputra basin, at ~25 km spatial resolution over 5 years, 2003–2007. The method applied here is based on the combination of surface water extent from a multi-satellite technique (GIEMS) and water bodies level height variations from

radar altimetry. A total of 58 time series of water level variations were constructed using the ENVISAT radar altimeter observations over the Ganges and Brahmaputra Rivers. A direct comparison with *in situ* river level variations at two stations, Hardinge on the Ganges and Bahadurabad on the Brahmaputra, confirms that ENVISAT radar altimeter can adequately monitor the river stage variations of these two rivers.

The new estimates of monthly SWS show realistic spatial distribution over the entire GB. The associated temporal variations exhibit a strong seasonal cycle and substantial interannual variability. The mean annual amplitude of ~410 km^3 in SWS over the GB Basin contributes to approximately 45% of the annual variations of GRACE-derived TWS. Annual SWS is estimated to be ~300 km^3 and ~250 km^3 for the Ganges and Brahmaputra Basin, respectively. The monthly SWS variations for the period 2003–2007 are evaluated against other related hydrological variables such as satellite-derived river discharge, precipitation and GRACE observations, showing that the seasonal and interannual variations agree well among all variables. We demonstrate that this new dataset can help in quantifying the surface water deficit during an extreme hydrological year. We estimate that the SWS deficit over the entire GB basin in July–August–September 2006 was about 30% as compared to other years.

Finally, the new SWS product can be used to separate the individual contribution of GRACE-derived TWS, such as isolating the variations of subsurface water storage (SSWS) (groundwater + soil moisture). We disaggregate the GRACE-derived TWS over the GB Basin for the period of 2003–2007 and find that the mean annual amplitude of SSWS of the entire basin is ~550 km^3. When reliable estimates of soil moisture storage change become available from satellite observations or hydrological model outputs, our results will also help estimate the GWS variations over the GB basin. Bringing together all these hydrological variables with estimates of river discharge, rainfall and surface evaporation will improve our knowledge on different water storage components and their contributions toward the terrestrial water budget over the GB Basin (Azarderakhsh et al., 2011).

This new and unique surface water storage and sub-surface water storage datasets for the GB basin over 5 years is a step toward a better understanding of hydrological and climate processes in the Indian Subcontinent region and their interactions with human activities (we note these datasets will be updated until present in the near future when global land surface emissivities become available along with the new CNES-ISRO radar altimeter AltiKa). In particular, this new dataset will help better characterize the continental processes during extreme events such as exceptional droughts in the GB basin, as well as to better quantify the causes and impacts of the actual "groundwater depletion" observed in the region.

Regarding satellite observations, our new dataset will play a key-role in the definition and validation of future hydrology-oriented satellite missions such as the NASA-CNES SWOT (Surface Water and Ocean Topography) dedicated to surface hydrology (Alsdorf et al., 2007; Papa et al., 2012).

Finally, surface freshwater storage is crucial to understand the role of continental water in the global and regional water cycle and present global sea level rise. Despite recent progress to quantify the two primary contributors to global sea-level rise – namely thermal expansion due to ocean warming and melting glaciers and ice sheets, large uncertainties still remain regarding the impact of changes in continental water storage on global and regional sea levels. Our estimates of SWS variations can be extended over the entire ISC in order to better quantify fluctuations in freshwater flux to the ocean, and to better understand the role of terrestrial water in the continent–ocean interactions and its impact on regional sea-level rise and variability over the Northern Indian Ocean (Ramilien et al., 2008; Pokhrel et al., 2012; Wada et al., 2012).

Conflict of interest

None declared.

Acknowledgments

This work is supported by the CNES-TOSCA and OST-ST grants 'Variability of terrestrial freshwater storage in the Tropics from multi-satellite observations'. This work is also supported in part by the

proposal BAND-AID (funded by the Belmont Forum and G8 Research Councils Initiative on Multilateral Research Funding) lead by C. K. Shum from the Ohio State University.

References

Adam, L., Döll, P., Prigent, C., Papa, F., 2010. Global-scale analysis of satellite-derived time series of naturally inundated areas as a basis for floodplain modeling. Adv. Geosci. 27, 45–50, http://dx.doi.org/10.5194/adgeo-27-45-2010

Aires, F., Papa, F., Prigent, C., 2013. A long-term, high-resolution wetland dataset over the Amazon basin, downscaled from a multi-wavelength retrieval using SAR. J. Hydrometeorol. 14, 594–607, http://dx.doi.org/10.1175/JHM-D-12-093.1

Alsdorf, D.E., Rodríguez, E., Lettenmaier, D.P., 2007. Measuring surface water from space. Rev. Geophys. 45, RG2002, http://dx.doi.org/10.1029/2006RG000197

Armstrong, R.L., Brodzik, M.J., 2005. Northern Hemisphere EASE-Grid Weekly Snow Cover and Sea Ice Extent Version 3. National Snow and Ice Data Center, Boulder, CO, USA.

Asada, H., Matsumoto, J., 2009. Effects of rainfall variation on rice production in the Ganges–Brahmaputra Basin. Clim. Res. 38, 249–260.

Azarderakhsh, M., Rossow, W.B., Papa, F., Norouzi, H., Khanbilvardi, R., 2011. Diagnosing water variations within the Amazon basin using satellite data. J. Geophys. Res. 116, D24107, http://dx.doi.org/10.1029/2011JD015997

Babel, M.S., Wahid, S.M., 2008. Freshwater Under Threat South Asia: Vulnerability Assessment of Freshwater Resources to Environmental Change. United Nations Environment Programme, Nairobi.

Birkett, C.M., 1995. The contribution of TOPEX/POSEIDON to the global monitoring of climatically sensitive lakes. J. Geophys. Res. 100 (C12), 25179–25204.

Birkett, C.M., Mertes, L.A.K., Dunne, T., Costa, M.H., Jasinski, M.J., 2002. Surface water dynamics in the Amazon Basin: application of satellite radar altimetry. J. Geophys. Res. 107 (D20), 8059–8080.

Bousquet, P., Ciais, P., Miller, J.B., Dlugokencky, E.J., Hauglustaine, D.A., Prigent, C., Van der Werf, G.R., Peylin, P., Brunke, E.G., Carouge, C., Langenfelds, R.L., Lathière, J., Papa, F., Ramonet, M., Schmidt, M., Steele, L.P., Tyler, S.C., White, J., 2006. Contribution of anthropogenic and natural sources to atmospheric methane variability. Nature 443, 439–443, http://dx.doi.org/10.1038/nature05132

Calmant, S., Seyler, F., Cretaux, J.F., 2008. Monitoring continental surface waters by satellite altimetry. Survey Geophys. 29, 247–269.

Chahine, M., 1992. The hydrological cycle and its influence on climate. Nature 359, 373–380.

Chowdhury, M.D.R., Ward, N., 2004. Hydro-meteorological variability in the greater Ganges–Brahmaputra–Meghna basins. Int. J. Climatol. 24, 1495–1508, http://dx.doi.org/10.1002/joc.1076

Crétaux, J.F., Kouraev, A.V., Papa, F., Bergé-Nguyen, M., Cazenave, A., Aladin, N., Plotnikov, I.S., 2005. Evolution of sea level of the big Aral Sea from satellite altimetry and its implications for water balance. J. Great Lakes Res. 31, 520–534.

Dai, A., Qian, T., Trenberth, K.E., 2009. Changes in continental freshwater discharge from 1948 to 2004. J. Clim. 22 (10), 2773–2792, http://dx.doi.org/10.1175/2008JCLI2592.1

Decharme, B., Douville, H., Prigent, C., Papa, F., Aires, F., 2008. A new river flooding scheme for global climate applications: off-line validation over South America. J. Geophys. Res. 113, D11110, http://dx.doi.org/10.1029/2007JD009376

Decharme, B., Alkama, R., Papa, F., Faroux, S., Douville, H., Prigent, C., 2012. Global off-line evaluation of the ISBA-TRIP flood model. Clim. Dyn. 38 (7–8), 1389–1412, http://dx.doi.org/10.1007/s00382-011-1054-9

Frappart, F., Seyler, F., Martinez, J.M., León, J.G., Cazenave, A., 2005. Floodplain water storage in the Negro River basin estimated from microwave remote sensing of inundation area and water levels. Remote Sens. Environ. 99, 387–399, http://dx.doi.org/10.1016/j.rse.2005.08.016

Frappart, F., Calmant, S., Cauhopé, M., Seyler, F., Cazenave, A.A., 2006. Preliminary results of ENVISAT RA-2 derived water levels validation over the Amazon basin. Remote Sens. Environ. 100, 252–264.

Frappart, F., Papa, F., Famiglietti, J.S., Prigent, C., Rossow, W.B., Seyler, F., 2008. Interannual variations of river water storage from a multiple satellite approach: a case study for the Rio Negro River basin. J. Geophys. Res. 113, D21104, http://dx.doi.org/10.1029/2007JD009438

Frappart, F., Papa, F., Güntner, A., Werth, S., Ramillien, G., Prigent, C., Rossow, W.B., Bonnet, M.-P., 2010. Interannual variations of the terrestrial water storage in the Lower Ob' Basin from a multisatellite approach. Hydrol. Earth Syst. Sci. 14, 2443–2453, http://dx.doi.org/10.5194/hess-14-2443-2010

Frappart, F., Ramillien, G., Maisongrande, P., Bonnet, M.-P., 2010b. Denoising satellite gravity signals by independent component analysis. IEEE Geosci. Remote Sens. Lett. 7 (3), 421–425, http://dx.doi.org/10.1109/LGRS.2009.2037837

Frappart, F., Papa, F., Güntner, A., Werth, S., Santos da Silva, J., Tomasella, J., Seyler, F., Prigent, C., Rossow, W.B., Calmant, S., Bonnet, M.-P., 2011. Satellite-based estimates of groundwater storage variations in large drainage basins with extensive floodplains. Remote Sens. Environ. 115, 1588–1594, http://dx.doi.org/10.1016/j.rse.2011.02.003

Frappart, F., Ramillien, G., Leblanc, M., Tweed, S.O., Bonnet, M.-P., Maisongrande, P., 2011b. An independent component analysis approach for filtering continental hydrology in the GRACE gravity data. Remote Sens. Environ. 115 (1), 187–204, http://dx.doi.org/10.1016/j.rse.2010.08.017

Frappart, F., Papa, F., Santos da Silva, J., Ramillien, G., Prigent, C., Seyler, F., Calmant, S., 2012. Surface freshwater storage and dynamics in the Amazon basin during the 2005 exceptional drought. Environ. Res. Lett. 7 (044010), http://dx.doi.org/10.1088/1748-9326/7/4/044010, 7 pp.

Fu, L.L., Cazenave, A., 2001. Satellite Altimetry and Earth sciences, A Handbook of Techniques and Applications. International Geophysics Series, vol. 69. Academic Press, San Diego.

Gain, A.K., Wada, Y., 2014. Assessment of future water scarcity at different spatial and temporal scales of the Brahmaputra River Basin. Water Resour. Manage., http://dx.doi.org/10.1007/s11269-014-0530-5

Getirana, A., Boone, A., Yamazaki, D., Decharme, B., Papa, F., Mognard, N., 2012. The hydrological modeling and analysis platform (HyMAP): evaluation in the Amazon basin. J. Hydrometeorol. 13, 1641–1665, http://dx.doi.org/10.1175/JHM-D-12-021.1

Han, S.-C., Kim, H., Yeo, I.-Y., Yeh, P., Oki, T., Seo, K.-W., Alsdorf, D., Luthcke, S.B., 2009. Dynamics of surface water storage in the Amazon inferred from measurements of inter-satellite distance change. Geophys. Res. Lett. 36, L09403, http://dx.doi.org/10.1029/2009GL037910
Hoekstra, A.Y., Mekonnen, M.M., Chapagain, A.K., Mathews, R.E., Richter, B.D., 2012. Global monthly water scarcity: blue water footprints versus blue water availability. PLoS ONE 7 (2), e32688.
Hoque, M.A., Hoque, M.M., Ahmed, K.M., 2007. Declining groundwater level and aquifer dewatering in Dhaka metropolitan area, Bangladesh: causes and quantification. Hydrogeol. J. 15, 1523–1534.
Huffmann, G.J., Adler, R.F., Bolvin, D.T., Gu, G., Nelkin, E.J., Bowman, K.P., Hong, Y., Stocker, E.F., Wolf, D.B., 2007. The TRMM multi-satellite precipitation analysis (TMPA): Quasi-global, multi-year, combined-sensor precipitation estimates at fine scale. J. Hydrometeorol. 8, 38–55.
Kalnay, E., Kanamitsu, M., Kistler, R., et al., 1996. The NCEP/NCAR 40-year reanalysis project. Bull. Am. Meteorol. Soc. 77, 437–470.
Kim, H., Yeh, P.J.-F., Oki, T., Kanae, S., 2009. Role of rivers in the seasonal variations of terrestrial water storage over global basins. Geophys. Res. Lett. 36, L17402, http://dx.doi.org/10.1029/2009GL039006
Konikow, L.F., Kendy, E., 2005. Groundwater depletion: a global problem. Hydrogeol. J. 13, 317–320.
Kundzewicz, Z.W., Mata, L.J., Arnell, N.W., Döll, P., Kabat, P., Jiménez, B., Miller, K.A., et al., 2007. Freshwater resources and their management. In: Parry, M.L., Canziani, O.F., Palutikof, J.P., van der Linden, P.J., Hanson, C.E. (Eds.), Climate Change 2007: Impacts, Adaptation, and Vulnerability. Contribution of Working Group II to the Fourth Assessment Report of the Intergovernmental Panel on Climate Change. Cambridge University Press, Cambridge, pp. 173–210.
Landerer, F.W., Swenson, S.C., 2012. Accuracy of scaled GRACE terrestrial water storage estimates. Water Resour. Res. 48, W04531, http://dx.doi.org/10.1029/2011WR011453
Lehner, B., Doell, P., 2004. Development and validation of a global database of lakes, reservoirs and wetlands. J. Hydrol. 296, 1–22.
Pandey, K.R., Crétaux, J.-F., Bergé-Nguyen, M., Tiwari, V.M., Drolon, V., Papa, F., Calmant, S., 2014. Water level estimation by remote sensing for the 2008 flooding of the Kosi River. Int. J. Remote Sens. 35 (2), 424–440, http://dx.doi.org/10.1080/01431161.2013.870678
Papa, F., Prigent, C., Durand, F., Rossow, W.B., 2006. Wetland dynamics using a suite of satellite observations: a case study of application and evaluation for the Indian Subcontinent. Geophys. Res. Lett. 33, L08401, http://dx.doi.org/10.1029/2006GL025767
Papa, F., Prigent, C., Rossow, W.B., 2007. Ob' River flood inundations from satellite observations: a relationship with winter snow parameters and river runoff. J. Geophys. Res. 112, D18103, http://dx.doi.org/10.1029/2007JD008451
Papa, F., Güntner, A., Frappart, F., Prigent, C., Rossow, W.B., 2008a. Variations of surface water extent and water storage in large river basins: a comparison of different global data sources. Geophys. Res. Lett. 35, L11401, http://dx.doi.org/10.1029/2008GL033857
Papa, F., Prigent, C., Rossow, W.B., 2008b. Monitoring flood and discharge variations in the large Siberian rivers from a multi-satellite technique. Surv. Geophys. 29 (4–5), 297–317, http://dx.doi.org/10.1007/s10712-008-9036-0
Papa, F., Prigent, C., Rossow, W.B., Matthews, E., 2010a. Interannual variability of surface water extent at global scale, 1993–2004. J. Geophys. Res. 115, D12111, http://dx.doi.org/10.1029/2009JD012674
Papa, F., Durand, F., Rossow, W.B., Rahman, A., Bala, S.K., 2010b. Satellite altimeter-derived monthly discharge of the Ganga–Brahmaputra River and its seasonal to interannual variations from 1993 to 2008. J. Geophys. Res. 115, C12013, http://dx.doi.org/10.1029/2009JC006075
Papa, F., Biancamaria, S., Lion, C., Rossow, W.B., 2012. Uncertainties in mean river discharge estimates associated with satellite altimeters temporal sampling intervals: a case study for the annual peak flow in the context of the future SWOT hydrology mission. IEEE Geosci. Remote Sens. Lett. 9 (4), 569–573, http://dx.doi.org/10.1109/LGRS.2011.2174958
Papa, F., Bala, S.K., Kumar Pandey, R., Durand, F., Gopalakrishna, V.V., Rahman, A., Rossow, W.B., 2012a. Ganga–Brahmaputra river discharge from Jason-2 radar altimetry: an update to the long-term satellite-derived estimates of continental freshwater forcing flux into the Bay of Bengal. J. Geophys. Res. 117, C11021, http://dx.doi.org/10.1029/2012JC008158
Papa, F., Frappart, F., Güntner, A., Prigent, C., Aires, F., Getirana, A.C.V., Maurer, R., 2013. Surface freshwater storage and variability in the Amazon basin from multi-satellite observations, 1993–2007. J. Geophys. Res. Atmos. 118, 11951–11965, http://dx.doi.org/10.1002/2013JD020500
Pavlis, N.K., Holmes, S.A., Kenyon, S.C., Factor, J.K., Paper presented at General Assembly 2008. An Earth gravitational model to degree 2160: EGM2008. Eur. Geophys. Union, Vienna, Austria.
Pedinotti, V., Boone, A., Decharme, B., Cretaux, J.F., Mognard, N., Panthou, G., Papa, F., Tanimoun, B.A., 2012. Evaluation of the ISBA-TRIP continental hydrologic system over the Niger basin using in situ and satellite derived datasets. Hydrol. Earth Syst. Sci. 16, 1745–1773, http://dx.doi.org/10.5194/hess-16-1745-2012
Pokhrel, Y.N., Hanasaki, N., Yeh, P.J.F., Yamada, T.J., Kanae, S., Oki, T., 2012. Model estimates of sea level change due to anthropogenic impacts on terrestrial water storage. Nat. Geosci. 5, 389–392, http://dx.doi.org/10.1038/ngeo1476
Prigent, C., Rossow, W.B., Matthews, E., 1997. Microwave land surface emissivities estimated from SSM/I observations. J. Geophys. Res. 102, 21867–21890.
Prigent, C., Matthews, E., Aires, F., Rossow, W.B., 2001. Remote sensing of global wetland dynamics with multiple satellite datasets. Geophys. Res. Lett. 28, 4631–4634, http://dx.doi.org/10.1029/2001GL013263
Prigent, C., Aires, F., Rossow, W.B., 2006. Land surface microwave emissivities over the globe for a decade. Bull. Am. Meteorol. Soc., 1573–1584, http://dx.doi.org/10.1175/BAMS-87-11-1573
Prigent, C., Papa, F., Aires, F., Rossow, W.B., Matthews, E., 2007. Global inundation dynamics inferred from multiple satellite observations, 1993–2000. J. Geophys. Res. 112, D12107, http://dx.doi.org/10.1029/2006JD007847
Prigent, C., Papa, F., Aires, F., Jimenez, C., Rossow, W.B., Matthews, E., 2012. Changes in land surface water dynamics since the 1990s and relation to population pressure. Geophys. Res. Lett. 39, L08403, http://dx.doi.org/10.1029/2012GL051276
Ramilien, G., Bouhours, S., Lombard, A., Cazenave, A., Flechtner, F., Schmidt, R., 2008. Land water storage contribution to sea level from GRACE geoid data over 2003–2006. Glob. Planet Change 60, 381–392, http://dx.doi.org/10.1016/j.gloplacha.2007.04.002
Ramillien, G., Frappart, F., Cazenave, A., Güntner, A., 2005. Time variations of the land water storage from an inversion of 2 years of GRACE geoids. Earth Planet. Sci. Lett. 235, 283–301.

Ringeval, B., de Noblet-Ducoudré, N., Ciais, P., Bousquet, P., Prigent, C., Papa, F., Rossow, W.B., 2010. An attempt to quantify the impact of changes in wetland extent on methane emissions at the seasonal and interannual time scales. Global Biochem. Cycles 24, GB2003, http://dx.doi.org/10.1029/2008GB003354

Ringeval, B., Decharme, B., Piao, S., Ciais, P., Papa, F., et al., 2012. Modelling sub-grid soil moisture saturation in the ORCHIDEE global land surface model: evaluation against river discharges and remotely sensed data. Geosci. Model Dev. 5, 941–962, http://dx.doi.org/10.5194/gmd-5-941-2012

Rodell, M., Velicogna, I., Famiglietti, J.S., 2009. Satellite-based estimates of groundwater depletion in India. Nature 460, 999–1003.

Rossow, W.B., Schiffer, R.A., 1999. Advances in understanding clouds from ISCCP. Bull. Am. Meteorol. Soc. 80, 2261–2287.

Santos da Silva, J., Calmant, S., Seyler, F., Filho, O.C.R., Cochonneau, G., Mansur, Webe J., 2010. Water levels in the Amazon basin derived from the ERS 2 and ENVISAT radar altimetry missions. Remote Sens. Environ. 114 (2010), 2160–2181.

Santos da Silva, J., Seyler, F., Calmant, S., Filho, O.C.R., Roux, E., Magalhães Araújo, A.A., Guyot, J.-L., 2012. Water level dynamics of Amazon wetlands at the watershed scale by satellite altimetry. Int. J. Remote Sens. 33 (11), 3323–3353, http://dx.doi.org/10.1080/01431161.2010.531914

Sengupta, D., Bharath Raj, G.N., Shenoi, S.S.C., 2006. Surface freshwater from Bay of Bengal runoff and Indonesian throughflow in the tropical Indian Ocean. Geophys. Res. Lett. 33, L22609, http://dx.doi.org/10.1029/2006GL027573

Shamsudduha, M., Uddin, A., 2007. Quaternary shoreline shifting and hydrogeologic influence on the distribution of groundwater arsenic in aquifers of the Bengal basin. J. Asian Earth Sci. 31 (2), 177–194.

Shamsudduha, M., Chandler, R.E., Taylor, R.G., Ahmed, K.M., 2009. Recent trends in groundwater levels in a highly seasonal hydrological system: the Ganges–Brahmaputra–Meghna Delta. Hydrol. Earth Syst. Sci. 13 (12), 2373–2385.

Shamsudduha, M., Taylor, R.G., Ahmed, K.M., Zahid, A., 2011. The impact of intensive groundwater abstraction on recharge to a shallow regional aquifer system: evidence from Bangladesh. Hydrogeol. J. 19 (4), 901–916.

Shamsudduha, M., Taylor, R.G., Longuevergne, L., 2012. Monitoring groundwater storage changes in the highly seasonal humid tropics: validation of GRACE measurements in the Bengal Basin. Water Resour. Res. 48, W02508, http://dx.doi.org/10.1029/2011WR010993

Tapley, B.D., Bettadpur, S., Ries, J.C., Thompson, P.F., Watkins, M., 2004. GRACE measurements of mass variability in the earth system. Science 305, 503–505.

Tiwari, V.M., Wahr, J., Swenson, S., 2009. Dwindling groundwater resources in northern India, from satellite gravity observations. Geophys. Res. Lett. 36, L18401, http://dx.doi.org/10.1029/2009GL039401

Wada, Y., Van Beek, L.P.H., Weiland, F.C.S., Cha, B.F., Wu, Y.H., Bierkens, M.F.P., 2012. Past and future contribution of global groundwater depletion to sea-level rise. Geophys. Res. Lett. 39, L09402.

Yamazaki, D., Kanae, S., Kim, H., Oki, T., 2011. A physically based description of floodplain inundation dynamics in a global river routing model. Water Resour. Res. 47, W04501, http://dx.doi.org/10.1029/2010WR009726

Zelli, C., 1999. ENVISAT RA-2 advanced radar altimeter: instrument design and pre-launch performance assessment review. Acta Astronaut. 44, 323–333.